A Trapped Intracellular Cation Modulates K^+ Channel Recovery From Slow Inactivation

Evan C. Ray and Carol Deutsch

Department of Physiology, University of Pennsylvania, Philadelphia, PA 19104

Upon depolarization, many voltage-gated potassium channels undergo a time-dependent decrease in conductance known as inactivation. Both entry of channels into an inactivated state and recovery from this state govern cellular excitability. In this study, we show that recovery from slow inactivation is regulated by intracellular permeant cations. When inactivated channels are hyperpolarized, closure of the activation gate traps a cation between the activation and inactivation gates. The identity of the trapped cation determines the rate of recovery, and the ability of cations to promote recovery follows the rank order $K^+ > NH_4^+ > Rb^+ > Cs^+ >> Na^+$, TMA. The striking similarity between this rank order and that for single channel conductance suggests that these two processes share a common feature. We propose that the rate of recovery from slow inactivation is determined by the ability of entrapped cations to move into a binding site in the channel's selectivity filter, and refilling of this site is required for recovery.

The Journal of General Physiology

INTRODUCTION

Voltage-gated potassium (K_V) channels are elegantly designed to function as negative feedback regulators of membrane potential. This role is critical for repolarization of the action potential in excitable cells. Once opened by depolarization, many K_V channels undergo a time-dependent decrease in conductance known as inactivation. Entry into, and recovery from, inactivated states determines the amount of K^+ conductance available to maintain cells at a negative resting membrane potential.

At least two mechanisms contribute to K^+ channel inactivation. N-type, or fast, inactivation occurs within milliseconds of activation as the channel's cytosolic N terminus occludes the pore, blocking the passage of K^+ ions through the channel (Hoshi et al., 1990; Zagotta and Aldrich, 1990). A second inactivation process occurs in response to sustained depolarization (Hoshi et al., 1991). It involves a localized rearrangement at the outer mouth of the channel (Choi et al., 1991; Yellen et al., 1994; Liu et al., 1996; Ogielska and Aldrich, 1999; Larsson and Elinder, 2000), including the outer portion of the channel's selectivity filter (Starkus et al., 1997; Harris et al., 1998; Ogielska and Aldrich, 1999). Rates associated with this process are typically slower than N-type inactivation; thus it is commonly referred to as slow inactivation.

Several factors affect entry into the slow inactivated state. First, both the concentration and species of cations present influence the rate of entry. Increased concentrations of permeant cations decrease the rate of slow inactivation (Grissmer and Cahalan, 1989a; Lopez-Barneo et al., 1993; Baukrowitz and Yellen, 1995, 1996; Kiss and Korn, 1998; Fedida et al., 1999). The ability of different species of cations to decrease the rate of slow inactivation corresponds approximately to the ability of these cations to permeate the channel (Lopez-Barneo et al., 1993). Second, intracellular blockers accelerate entry into the slow inactivated state (Armstrong, 1969; Hoshi et al., 1991; Baukrowitz and Yellen, 1995; Rasmusson et al., 1995; Loots and Isacoff, 1998), suggesting that slow inactivation is facilitated by preventing the replacement of an outwardly exiting pore K^+ with a K^+ ion from the internal solution (Baukrowitz and Yellen, 1996). These observations attest to a relationship between permeation and inactivation gating and support the suggestion that occupancy of cation binding sites in the permeation pathway inhibits closure of the inactivation gate (Lopez-Barneo et al., 1993). This is a version of the "foot-in-the-door" mechanism invoked to explain the influence of monovalent cations on activation-gate closure (Swenson and Armstrong, 1981).

After inactivation, membrane hyperpolarization favors exit from the inactivated state via a gating process referred to as recovery. This process is at least as important as entry into the inactivated state in determining the number of conductive channels available to a cell. It is this availability that contributes critically to generation of an action potential, the frequency of action potential firing, and repolarization of the membrane following an action potential. The physiological importance of recovery from slow inactivation is underscored by the finding that in some channels, even when fast inactivation is

Correspondence to Carol Deutsch: cjd@mail.med.upenn.edu

Abbreviations used in this paper: FR, fractional recovery; I, inactivated; NI, noninactivated; TMA, tetramethylammonium.

present, recovery from the slow inactivated state is still rate limiting in returning channels to a state from which they can be called upon to repolarize the cell (Rasmusson et al., 1995; Kurata et al., 2004). Although the detailed sequence of events involved in recovery from slow inactivation is not known, recovery, like entry into the inactivated state, depends on the interaction of the channel with permeant cations. Increased concentrations of extracellular cations speed the rate of recovery after slow inactivation (Pardo et al., 1992; Levy and Deutsch, 1996a,b; Rasmusson et al., 1998), and more conductive extracellular cations do so more effectively than less conductive cations (Levy and Deutsch, 1996a).

These precedents for modulation of gating kinetics by extracellular cations indicate that K_V channels possess extracellular cation-binding modulatory sites. However, occupancy of these sites is not the sole determinant of inactivation rate. Indeed, cation binding to more intracellular sites along the axis of permeation also influences inactivation (Fedida et al., 1999; Ogielska and Aldrich, 1999), an observation that has been suggested to occur as a result of electrostatic interaction between cations occupying inner and outer sites along the pore axis (Ogielska and Aldrich, 1999). Thus, cations at internal and external sites along the permeation pathway may act in concert to modulate the rate and extent of slow inactivation. Just as entry into the inactivated state is governed by the occupancy of cations at multiple sites, so too might occupancy of internal and external sites conspire to modulate exit from the inactivated state. Although several studies have characterized the influence of extracellular cations on recovery (Pardo et al., 1992; Rasmusson et al., 1995; Levy and Deutsch, 1996a,b), little is known about the effects of intracellular cations on this process. In this study, we examine the influence of intracellular cations on recovery. We find that when the activation gate of an inactivated channel closes, a cation from the intracellular solution becomes trapped between the intracellular end of the selectivity filter and the activation gate. This trapped cation interacts with a modulatory site in the filter to govern recovery rate. The rate of recovery depends on the identity of the trapped cation and correlates with conductance of the cation through the open channel. It is the nature of the trapped cation and its ability to jump from one site to another in the selectivity filter that is common to both the recovery process and conductance through the open channel. These findings reveal a new role for K^+ ions in occupying and stabilizing the conductive structure of a voltage-gated K^+ channel.

MATERIALS AND METHODS

Cell Culture

Human embryonic kidney cells transformed with SV40 large T antigen (tsA201) were grown in DMEM-high glucose supplemented with 10% FBS, 2 mM L-glutamine, 100 U/ml penicillin-G, and 100 μg/ml streptomycin (Invitrogen) at 37°C in a 9% CO_2 and 95% air humidified atmosphere. Cells were passaged twice per week after a 7-min incubation in Versene containing 0.2 g EDTA/L (Invitrogen).

DNA Clones and Site-directed Mutagenesis

Modified *Shaker*-IR in a GW1-CMV mammalian expression plasmid, under the control of a highly expressing Kozak consensus promoter sequence (Kozak, 1991), was provided by R. Horn (Thomas Jefferson University, Philadelphia, PA) (Ding and Horn, 2002). This construct includes a deletion of amino acids 6–46 to remove N-type inactivation, and C301S and C308S point mutations (Holmgren et al., 1996). Amino acid substitutions at position 449 were introduced using a QuikChange site-directed mutagenesis kit (Stratagene). Mutants were sequenced at the University of Pennsylvania School of Medicine DNA Sequencing Facility using an ABI 3100 16 capillary sequencing apparatus with BigDye Taq FS Terminator V 3.1 chemistry. A calcium phosphate transfection kit (Invitrogen) was used to cotransfect CD8 carried in an EBO-pcD vector (Margolskee et al., 1988; Margolskee et al., 1993) with a *Shaker*-IR 449 construct using 6 or 8 μg of CD8 or *Shaker*-IR DNA, respectively, per 100-ml dish of tsA201 cells. Transfected cells were replated onto Corning 35-mm polystyrene cell culture dishes either pretreated with poly-L-ornithine (Sigma-Aldrich) to improve cell adhesion for pulling patches or untreated for whole-cell patching. 12–36 h following transfection, current was recorded from transfected cells, which were identified by decoration with anti-CD8 antibody-coated Dynabeads (Dynal Biotech) as described previously (Margolskee et al., 1993; Jurman et al., 1994).

Electrophysiology

Standard methods were used to record Cs^+ currents in the whole-cell configuration and K^+ currents in outside-out patches. Perfusion experiments were performed on inside-out patches. Data were acquired using an Axopatch 200B amplifier with 10 kHz filtration (Axon Instruments, Inc.), digitized with a Digidata 1322A analogue-to-digital converter, and recorded with a 20-kHz sampling interval using Clampex (Axon Instruments, Inc.) on a personal computer (Dell). For whole-cell and outside-out experiments, electrodes of 1.6–2.2 MΩ resistance were pulled from SG10 leaded glass (Richland Glass). For inside-out patches, 8–11 MΩ pipettes were pulled from lead-free 8520 glass (Warner Instruments). Pipettes were coated with R-6101 elastomer (Essex Group, Inc.) and fire polished. Adjustments for bath–pipette liquid junction potentials were made before current recording. Whole-cell recordings were performed after a 10-min dialysis period to ensure equilibration of pipette and intracellular solutions. All holding potentials were −100, and voltage errors were <3 mV after series resistance compensation. All experiments were performed at room temperature (20–24°C). Data were analyzed using Clampfit (Axon Instruments, Inc.) and Igor (Wavemetrics, Inc.). Unless otherwise stated, reported errors are SEM.

Solutions

Standard intracellular solutions contained 105 XF, 35 XCl, 10 EGTA, 10 HEPES (X is the relevant cation and concentrations are given in mM), titrated to pH 7.36–7.38 with XOH, for a final concentration of 160–165 mM and osmolarity of 285–295 mOsm. Standard extracellular solution was 20 mM KCl, 1.5 $CaCl_2$, 1.0 $MgCl_2$, and 10 HEPES. Osmolarity was brought to 296–300 mOsm with NMG, and pH was titrated to 7.36–7.38 with HCl. For solutions with reduced test cation concentrations, osmolarity was maintained by the addition of an appropriate concentration of NMG. All chemicals were obtained from Fisher Scientific or Sigma-Aldrich.

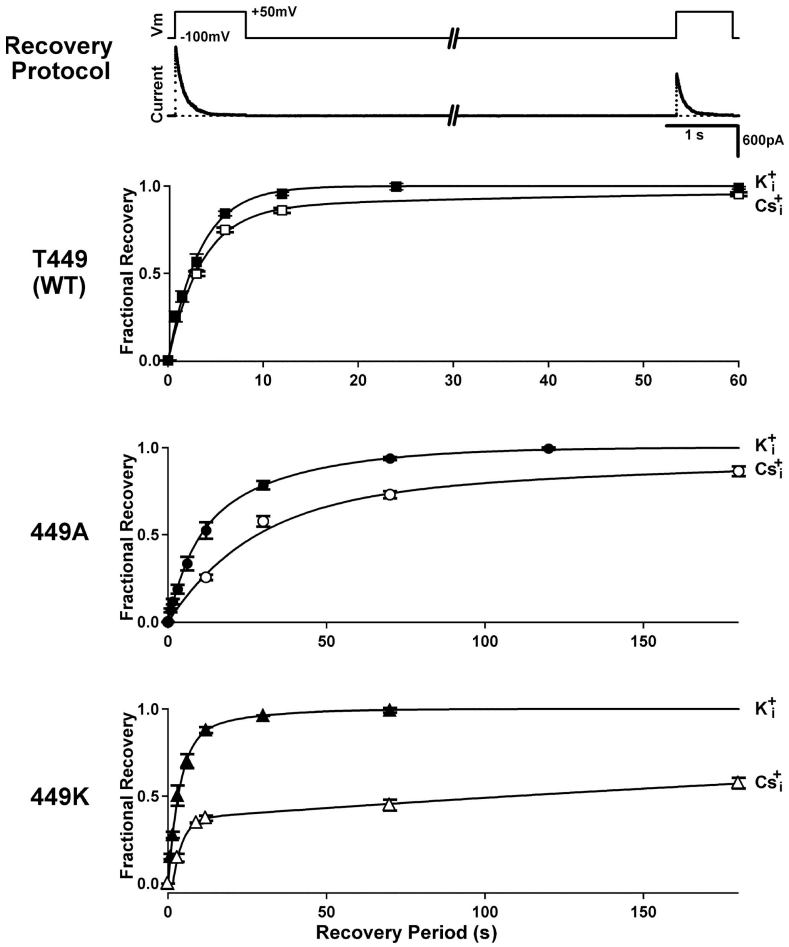

Figure 1. Rate of recovery depends on intracellular cation and 449-side chain. Recovery kinetics were examined by plotting fractional recovery (FR) of inactivated current with respect to time. Currents in 162 K^+_i were recorded using outside-out patches, whereas the drastically reduced conductance of 164Cs^+_i required that its currents be recorded in whole-cell configuration. For all recordings, K^+_o was 20 mM. (Top) The two-pulse protocol and representative current trace used to calculate FRs for 449A. The recovery period shown equals 12 s. (Below) Recovery time courses for T449, 449A, and 449K. Cs^+_i adds a slow phase to the recovery time course, an effect which is subtle in T449, more pronounced in 449A, and dramatic in 449K. Note that time scales differ for T449 vs. mutants. Equations used for fits and resulting coefficients are described in Table I. Data are means ± SEM (n = 3–7).

Recovery Measurements

To measure recovery, a standard two-step voltage protocol was used. Unless otherwise stated, voltage steps were to +50 mV. The duration of the first step used to inactivate channels and measure initial peak current amplitude was at least fivefold longer than the channel's time constant for inactivation. For longer pulses, recovery rates did not change as a function of pulse duration (not depicted). After a recovery period of variable length at −100 mV, the second voltage step was applied, and peak recovered current amplitude was measured. No leak subtraction was used. Fractional recovery (FR) was calculated as $(I_{rec} - I_{ss})/(I_o - I_{ss})$, where I_o, I_{rec}, and I_{ss} represent the peak current amplitudes during the first depolarizing step, the second depolarizing step, and the inactivated steady state, respectively (Levy and Deutsch, 1996a). In whole-cell recordings in Cs^+_i (Figs. 1–3), because peak Cs^+ current amplitude was not fully restored within a reasonable recovery period (≤20 min), no depolarizing step was applied during the initial 10-min dialysis period, after which a single two-pulse protocol was administered, and the cell was discarded.

Perfusion Experiments

Inside-out patches were perfused with standard intracellular solutions at a rate of 1 ml/min. The pipette solution contained standard 20 mM K^+ with NMG. Reversal potentials were measured on each patch to confirm complete perfusion. Solution switches were performed using a RSC-160 perfusion apparatus (Bio-Logic Science Instruments). On average, perfusion was >95% complete within 90 ms. Voltage protocols were modified to compensate for small liquid junction potentials arising from solution switching. To ensure full restoration of current between recovery measurements, patches were maintained at −100 mV in K^+_i for ≥4 min after depolarization in intracellular K^+. Statistical significance of differences in mean fractional recovery was determined using the Student-Newman-Keuls all pairwise multiple comparison procedure.

RESULTS

Intracellular Cs^+ Slows Recovery

To study the influence of intracellular permeant ions on recovery, we sought conditions in which recovery could be easily characterized, including conditions producing tractable inactivation and recovery rates. Although *Shaker*-IR inactivates, its relatively slow inactivation time constant (τ_{inact}) of 1.3 s in 2 mM extracellular K^+ is too large for convenient recovery measurements. In contrast, the *Shaker*-IR 449A and 449K mutants have a τ_{inact} of 160 and 40 ms, respectively (Lopez-Barneo et al., 1993). Therefore, we compared recovery time courses for *Shaker*-IR (T449), and mutants *Shaker*-IR 449A and *Shaker*-IR 449K. We believe this allows us to study the same inactivation process because, although it is possible that a 449 mutation fundamentally alters the mechanism of slow inactivation, there is no evidence

TABLE I

Recovery Kinetics

Mutant	Intracellular Cation	A_{fast}	τ_{fast} or τ_{rec} (s)	A_{slow}	τ_{slow} (s)
T449 (WT)	K^+ (6)	–	3.27 ± 0.14	–	–
	Cs^+ (3–4)	0.88 ± 0.06	3.46 ± 0.45	0.13 ± 0.06	62 ± 50
449A	K^+ (5)	0.47 ± 0.14	7.4 ± 2.0	0.53 ± 0.14	32.2 ± 4.9
	Cs^+ (3–6)	0.72 ± 0.12	26.6 ± 4.9	0.28 ± 0.12	240 ± 190
449K	K^+ (3)	0.87 ± 0.09	3.98 ± 0.87	0.13 ± 0.11	24 ± 16
	Cs^+ (3–7)	0.40 ± 0.03	4.8 ± 1.1	0.60 ± 0.03	530 ± 160

Time courses were fit with the double exponential function: $FR = 1 - [A_{slow}*\exp(-RP/\tau_{slow}) + A_{fast}*\exp(-RP/\tau_{fast})]$, where RP represents the recovery period, i.e., the time that channels were allowed to recover at the −100 mV holding potential; τ_{fast} and τ_{slow} represent the time constants for the fast and slow phases of the curve; and A_{slow} and A_{fast} denote the weight coefficients for each of these phases. When τ_{slow} and τ_{fast} did not differ significantly or A_{slow} was not significantly larger than 0, the time course was assumed to be monoexponential and was re-fit with the single exponential function $FR = 1 - \exp(-RP/\tau_{rec})$, where τ_{rec} represents the single exponential recovery time constant. For K^+_i, values in parentheses represent the number of patches from which a complete recovery time course was recorded. For Cs^+_i, no cell contributed more than one FR measurement, and values in parentheses represent the number of cells contributing to the FR for each point on the x axes shown in Fig. 1. The parameters and their errors were estimated by weighted chi-square minimization using data from all cells simultaneously. This was necessary because in some cells as few as one determination of recovery was made at a single RP.

to support this conjecture. Furthermore, 449 mutants exhibit at least one hallmark of slow inactivation: a dependence of inactivation rate and recovery rate (unpublished data) on extracellular $[K^+]$. Initially, we studied 449 mutants using K^+ or poorly permeant Cs^+ as the intracellular cation. The permeability ratio of these cations (P_{Cs}/P_K) is 0.10, and the conductance ratio (γ_{Cs}/γ_K) is 0.01 (Heginbotham and MacKinnon, 1993).

For these recovery measurements, 20 mM extracellular K^+ (K^+_o) was used because of the diminutive nature of Cs^+ currents through 449K channels in more dilute extracellular K^+ solutions. As shown in Fig. 1 and Table I, recovery consistently occurred more slowly in the presence of intracellular Cs^+ (Cs^+_i) than in intracellular K^+ (K^+_i). The degree to which recovery was slowed depended on the identity of the 449 side chain. T449 recovers quickly in K^+_i, and an exponential function fits the T449 recovery time course well, with $\tau_{rec} = 3.27 \pm 0.14$ s. Recovery of T449 occurred slightly more slowly in Cs^+_i and is better fit with a double-exponential function.

The mutants exhibit more dramatic phenotypes. 449A recovers with biphasic kinetics (Fig. 1; see also Meyer and Heinemann, 1997). This is true regardless of the identity of the intracellular cation (unpublished data). However, in the presence of Cs^+_i, the biphasic nature of the recovery time course becomes more pronounced, with τ_{slow} ~10-fold larger than τ_{fast}. In 449K, recovery is bi-exponential and even more dependent on the nature of the intracellular cation. When K^+ is present on both sides of the membrane ($K^+_o//K^+_i$), the time constants of the two recovery phases differ by less than fivefold. Replacement of K^+_i with Cs^+_i produces a dramatic slow phase with a weight coefficient, A_{slow}, of 0.60 ± 0.03, and a 100-fold difference in τ_{fast} and τ_{slow}. The prominent slow phase observed in Cs^+_i suggests that replacement of K^+_i with Cs^+_i causes a substantial fraction of channels to enter a more stable inactivated state in response to a sustained depolarizing voltage step.

Because binding of extracellular K^+ to inactivated K_v channels promotes recovery (Levy and Deutsch, 1996a,b), we asked whether slow recovery occurs merely as a consequence of removal of K^+_i, or as a result of the

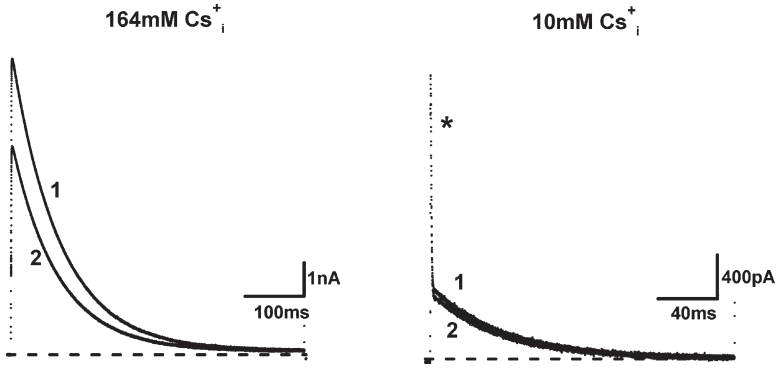

Figure 2. Reduction of intracellular Cs^+ speeds recovery. 449A current traces in response to a step to +50 mV are shown before (1) and after (2) a 90-s RP at −100 mV. Dashed gray line represents zero-current level. Reduction of Cs^+_i increased FR from 0.69 (in 164 mM Cs^+_i) to 0.90 (in 10 mM Cs^+_i). Addition of NMG^+ to the 10 mM Cs^+_i solution maintained osmolarity. K^+_o was 5 mM to maintain an outward driving force with both intracellular solutions. Decreased outward driving force in 10 mM Cs^+_i results in smaller ionic currents, allowing gating currents (*) to be readily observed. For the current traces shown, the inactivation time constants obtained in 164 and 10 mM Cs^+_i are 164 and 47 ms, respectively. The average time constants (±SEM) are 180 ± 17 ms ($n = 3$) and 47.3 ± 2.9 ms ($n = 4$), respectively.

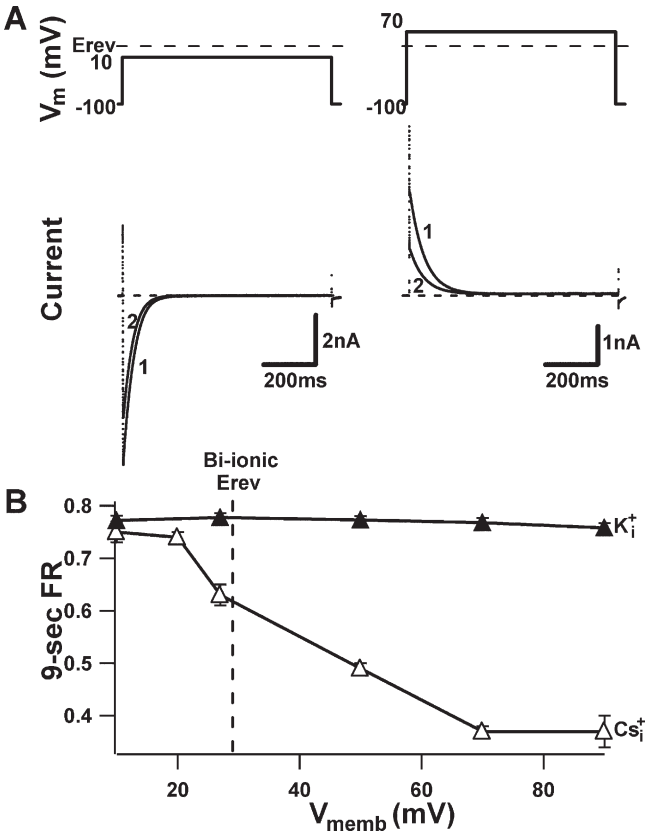

Figure 3. Dependence of FR on current direction. (A) Voltage protocols used in a two-pulse recovery whole-cell experiment to elicit currents through 449K in 20 K^+_o//80 Cs^+_i. Steps to test potentials less positive than E_{rev} (29 mV) produce inward currents, whereas potentials greater than E_{rev} produce outward currents. Voltage protocol and current recorded during a 10-mV (left) or 70-mV (right) depolarizing pulse. Trace 1 shows the original inactivating current; trace 2 shows current after a 9-s recovery period at −100 mV. (B) Fractional recoveries obtained as described in A in either 20 K^+_o//80 Cs^+_i (open triangles) or 20 K^+_o//80 K^+_i (filled triangles) were plotted versus depolarization pulse potential. (n = 3 for each K^+_o//K^+_i FR measurement, and n = 4–7 for each K^+_o//Cs^+_i measurement.) Error bars represent SEM.

presence of Cs^+_i. If recovery is slower in Cs^+_i simply due to K^+_i removal, then fractional recovery (FR) in the absence of K^+_i should not vary with Cs^+_i concentration. In contrast, if slow recovery were due to binding of Cs^+_i to the channel, then a reduction in Cs^+_i would speed recovery. We therefore compared fractional recoveries for 449A in 164 and 10 mM Cs^+_i, each in the absence of K^+_i. Fig. 2 shows current recordings during both pulses of a two-pulse recovery protocol in 164 mM Cs^+_i (left) and 10 mM Cs^+_i (right). In 164 mM Cs^+_i, a significantly smaller fraction of channels recovered than in 10 mM Cs^+_i after 90 s at −100 mV. Reduction of Cs^+_i increased FR from 0.68 ± 0.01 (in 164 mM Cs^+_i, n = 3) to 0.91 ± 0.02 (in 10 mM Cs^+_i, n = 5). The simplest explanation for this finding is that intracellular Cs^+ binds to a site within the channel and, in so doing, promotes slow recovery.

The Recovery Modulatory Site Resides in the Permeation Pathway

To determine whether the binding site lies in the permeation pathway, we examined the relationship between fractional recovery and direction of current flow in 449K using K^+_o//Cs^+_i. This mutant, as demonstrated by Fig. 1 and Table I, was the mutant of choice for all subsequent experiments. If the binding site lies in the permeation pathway, large outward currents that flood the pathway with Cs^+ would tend to retard recovery; large inward currents that flood the pathway with K^+ would speed recovery. In contrast, if the binding site for the modulatory cation resides outside the permeation pathway, recovery should be independent of current direction.

To manipulate current direction, the potential at which channels were inactivated was varied and the dependence of FR on inactivating potential was measured (Fig. 3). Cation concentrations (20 K^+_o//80 Cs^+_i) were chosen to render a positive reversal potential (E_{rev}, ~29 mV) so that FR could easily be measured at multiple test potentials on either side of E_{rev}. Potentials significantly more positive than E_{rev} resulted in outward Cs^+ currents with small FR (0.37 ± 0.03 at 70 mV). This FR resembled the value previously observed in 20 K^+_o//164 Cs^+_i at +50 mV (0.35 ± 0.01, Fig. 1). Fractional recovery increased after inactivation at potentials closer to E_{rev}. At potentials less positive than E_{rev}, large inward K^+ currents resulted, and FRs at 10 mV (0.75 ± 0.06) approached a maximum, similar to that observed in the 20 K^+_o//80 K^+_i control (0.77 ± 0.02 at 10 mV). Fractional recovery in 20 K^+_o//80 K^+_i showed no sensitivity to changes in inactivation potential, with similar FR after inactivation at 10 and 90 mV (0.76 ± 0.02 at 90 mV). Thus, FR is voltage dependent under bi-ionic conditions, consistent with a modulatory binding site within the permeation pathway. Alternatively, the recovery rate could be set intrinsically by the depolarized voltage that causes inactivation. However, this alternative interpretation fails to explain (1) the invariance of FRs obtained for channels bathed in bilateral K^+ (K^+_o//K^+_i) and depolarized to different potentials, (2) the striking similarity between FRs obtained for channels bathed in K^+_o//K^+_i and those bathed in bi-ionic solutions (20 K^+_o//80 Cs^+_i) at potentials allowing large inward currents, and (3) the presence of the reversal potential within the voltage range through which fractional recovery crosses between its extremes. We therefore favor the conclusion that the binding site (or sites) governing recovery resides within the permeation pathway.

Location of the Binding Site for Intracellular Cations

Where in this pathway does intracellular Cs^+ bind: on the intra- or extracellular side of the slow inactivation gate? For simplicity, we refer to the location of cation–channel interaction as a single binding site, although

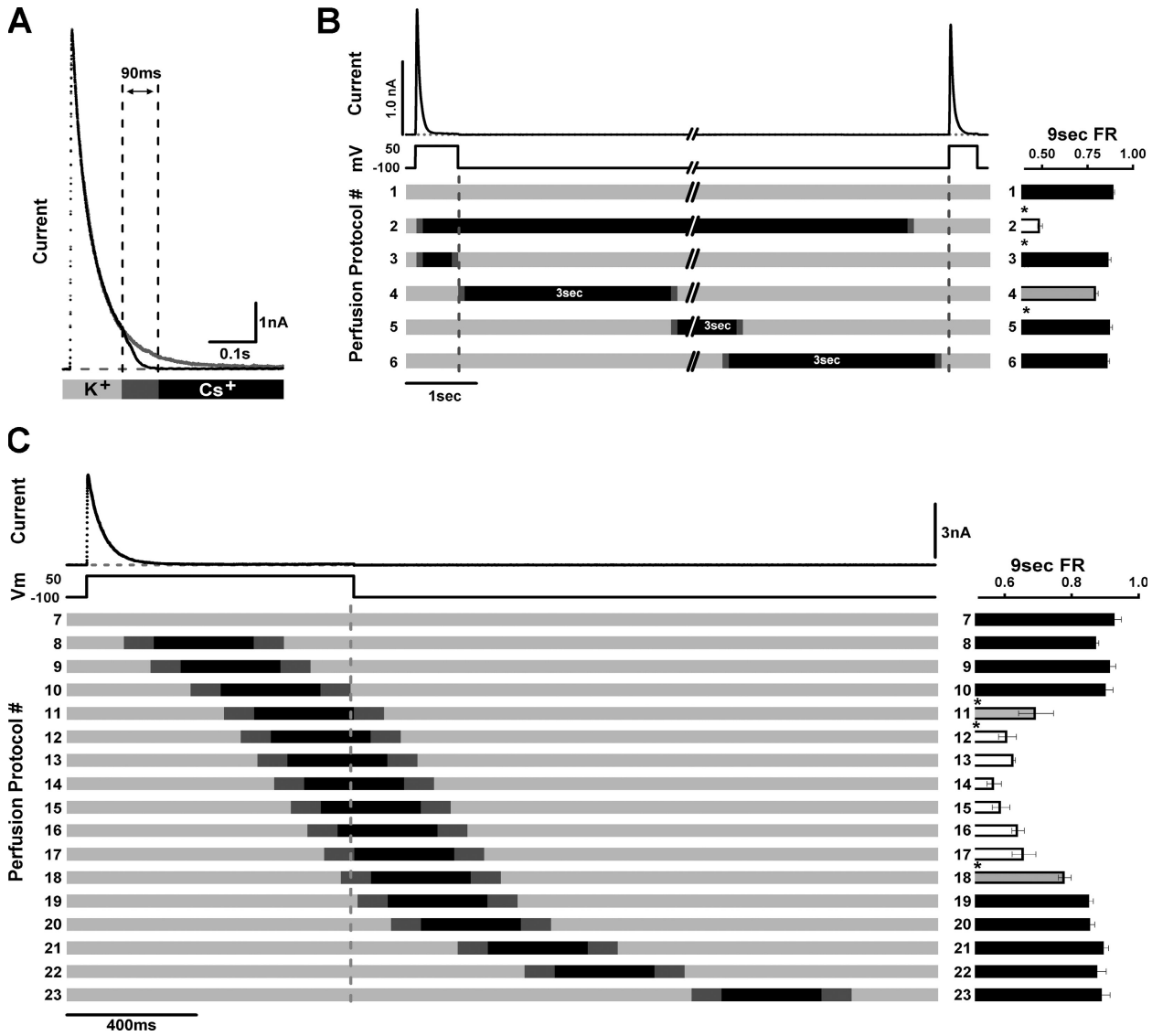

Figure 4. Pulses of intracellular Cs^+ reduce fractional recovery. Inside-out patches containing 449K with 20 K^+_o were perfused with 162 K^+_i or 164 Cs^+_i. (A) Shading scheme for perfusion kinetics. Channels were depolarized to +50 mV during perfusion with 162 K^+_i (light gray). After 110 ms, perfusion with 164 Cs^+_i was begun. As Cs^+_i replaces K^+_i, current drops to near zero as a consequence of lower Cs^+_i conductance (darker gray). Complete Cs^+_i perfusion was confirmed by E_{rev} determination (not depicted). For comparison, a Cs^+_i-free current trace is also plotted in gray. Periods of complete Cs^+_i perfusion are shown in black. (B) The influence of various Cs^+_i pulses on FR. Fractional recovery after a 9-s recovery period was measured after perfusion with Cs^+_i for different intervals during inactivation and recovery. The two-pulse protocol and current elicited in the absence of a Cs^+_i pulse are shown above. Schematized perfusion protocols employed are shown below, using the shading scheme from A. Protocol numbers are shown on either side of each schematic. Horizontal bars at right represent FR for the corresponding perfusion protocol (mean ± SEM, n = 5–9 for each FR measurement). Different shading in the bar graph shows significantly different statistical groups ($P < 0.05$). Adjacent pairs determined to be significantly different are noted with an asterisk. (C) 400-ms Cs^+_i pulses applied as channels return to −100 mV. For simplicity, only the first pulse and associated current of a two-pulse protocol are shown. Perfusion protocol shading scheme and bars representing FR (n = 4–6) are as in A and B.

this interaction may occur through multiple binding sites. To address this question, inside-out patches were subjected to pulses of Cs^+_i at various times during inactivation and recovery. If the cation binding site resides on the extracellular side of the inactivation gate, Cs^+_i must access that site before closure of the gate. Application of Cs^+_i before inactivation will slow recovery, whereas Cs^+_i application after inactivation will have no effect on recovery. If the binding site is present on the intracellular side of the inactivation gate and still accessible to Cs^+_i, a Cs^+_i pulse may suffice to slow recovery.

Three technical issues were considered in these experiments: (1) the solution exchange time for the pulsed applications, (2) the junction potentials induced by solution changes, and (3) ensuring complete recovery between protocols. The first two issues were addressed by

direct measurement (Fig. 4 A; Materials and Methods). Complete exchange (>95%), determined by E_{rev}, occurred within 90 ms, and voltage protocols included corrections for all junction potentials. The third issue was particularly relevant because multiple FR measurements were made with each inside-out patch. To allow channels to fully recover between protocols, patches were maintained at the holding potential (−100 mV) in K^+_i for a minimum of 4 min. Regardless of whether Cs^+_i was applied, the second test depolarization of the two-pulse protocol (applied in the presence of K^+_i) followed by a 4-min "reset" period (also in the presence of K^+_i), restored the original current amplitude. With these issues resolved, we proceeded to carry out the experiments shown in Fig. 4 (B and C) (Protocols 1–23).

When K^+_i was continuously applied to channels during a two-pulse protocol, a fraction of inactivated channels equal to 0.89 ± 0.01 recovered in 9 s (Protocol 1). However, when Cs^+_i perfusion was initiated 21 ms after the start of the depolarizing pulse and maintained for the majority of the recovery period, FR decreased to 0.49 ± 0.01 (Protocol 2). This observation confirms that an exposure of the channel to intracellular Cs^+ is sufficient to slow recovery, even when the peak current recorded is carried by K^+. A Cs^+_i pulse applied to open channels as their inactivation gates close, but terminated before the end of the depolarizing pulse (Protocol 3), resulted in FR of 0.87 ± 0.01, statistically indistinguishable (P = 0.45) from the FR obtained when K^+_i is present continuously. This finding suggests that the modulatory binding site does not reside on the extracellular side of the inactivation gate and is more likely to lie on the intracellular side. Moreover, if channels bind Cs^+ during the depolarization in Protocol 3, from either the open or the inactivated state, they rapidly release it at the end of the Cs^+_i pulse.

Indeed, if the modulatory site is on the intracellular side of the slow inactivation gate and accessible, then we expect application of Cs^+_i to inactivated channels to slow recovery. To test this hypothesis, we applied Cs^+_i to inactivated channels as they recovered from inactivation. In Protocols 4–6, Cs^+_i pulses were administered to inactivated channels during the initial, middle, or final third of a 9-s recovery period. No significant difference in FR occurred when Cs^+_i was applied during the middle (FR = 0.88 ± 0.01) or final (FR = 0.86 ± 0.01) thirds of the recovery period (P = 0.33 and 0.10, respectively). However, FR was slightly, but significantly, smaller when Cs^+_i was applied during the first third of the recovery period (FR = 0.80 ± 0.01, P < 0.01).

These results suggest that a period of sensitivity to Cs^+_i occurs soon after inactivated channels are returned to a hyperpolarized holding potential. To identify the specific time interval that is ion sensitive, we used overlapping Cs^+_i pulses of equal (~400 ms) duration applied before, during, and after the end of the first depolarizing pulse in a two-pulse protocol (Fig. 4 C). Cs^+_i pulses ending before the termination of the depolarizing pulse failed to reduce FR (Protocols 8–10), consistent with the results shown in Fig. 4 B. When Cs^+_i was present as channels returned to their holding potential, FR decreased significantly (Protocols 11–18), whereas later in the recovery period (>100 ms after the end of the depolarizing pulse), channels became insensitive to Cs^+_i (Protocols 19–23). Assuming that slow inactivation effectively bars access of intracellular Cs^+ to binding sites on the extracellular side of the inactivation gate, these results provide additional evidence that the modulatory binding site resides on the intracellular side of this gate.

To explain the decreased recovery that is manifest many seconds after a brief Cs^+_i pulse, we propose that an intracellular cation is trapped in the permeation pathway after return of a channel to its holding potential. In support of this hypothesis, the original current amplitude was completely restored between consecutive two-pulse protocols (allowing repeated FR measurements to be made on the same patch), suggesting that trapped Cs^+_i can be released by the second depolarization in a two-pulse protocol. To explicitly test whether depolarization releases the trapped Cs^+, we modified Protocol 14 shown in Fig. 4 C to include a 10-ms step to +50 mV after the Cs^+_i-to-K^+_i switch. This 10-ms step was sufficient to fully restore the FR to levels seen in the absence of a Cs^+_i pulse (Fig. 5 A). This suggests that a trapped Cs^+ continued to slow recovery, even after intracellular Cs^+ was washed away, and a liberation step during the recovery period released the trapped Cs^+. Consistent with this conclusion, a 10-ms step in the continued presence of Cs^+ does not restore FR, eliminating the possibility that depolarization itself restores FR.

A straightforward interpretation of this observation would be that depolarization opened the channel's activation gate, allowing trapped Cs^+ to be replaced with K^+ from the internal solution. If release of Cs^+ is dependent on opening of the activation gate, then recovery should be a function of activation-gate open probability (P_o) and the kinetics of Cs^+ liberation should correlate with the kinetics of activation. To test this hypothesis, we compared recovery after liberation voltage steps to two different voltages, 0 and +80 mV. At these voltages, the channel has markedly different activation kinetics, activating more slowly at 0 mV than at +80 mV. We measured FR as a function of liberation-step duration and compared this to activation rates of the channel from a holding potential of −100 mV to 0 or +80 mV. At +80 mV, Cs^+ liberation kinetics bore a striking resemblance to those of channel activation at the same potential, even faithfully recapitulating the sigmoidal delay in *Shaker*'s activation time course (Hoshi et al., 1994; Zagotta et al., 1994a; Zagotta et al., 1994b). This agreement suggests that the rate-limiting step in Cs^+ liberation

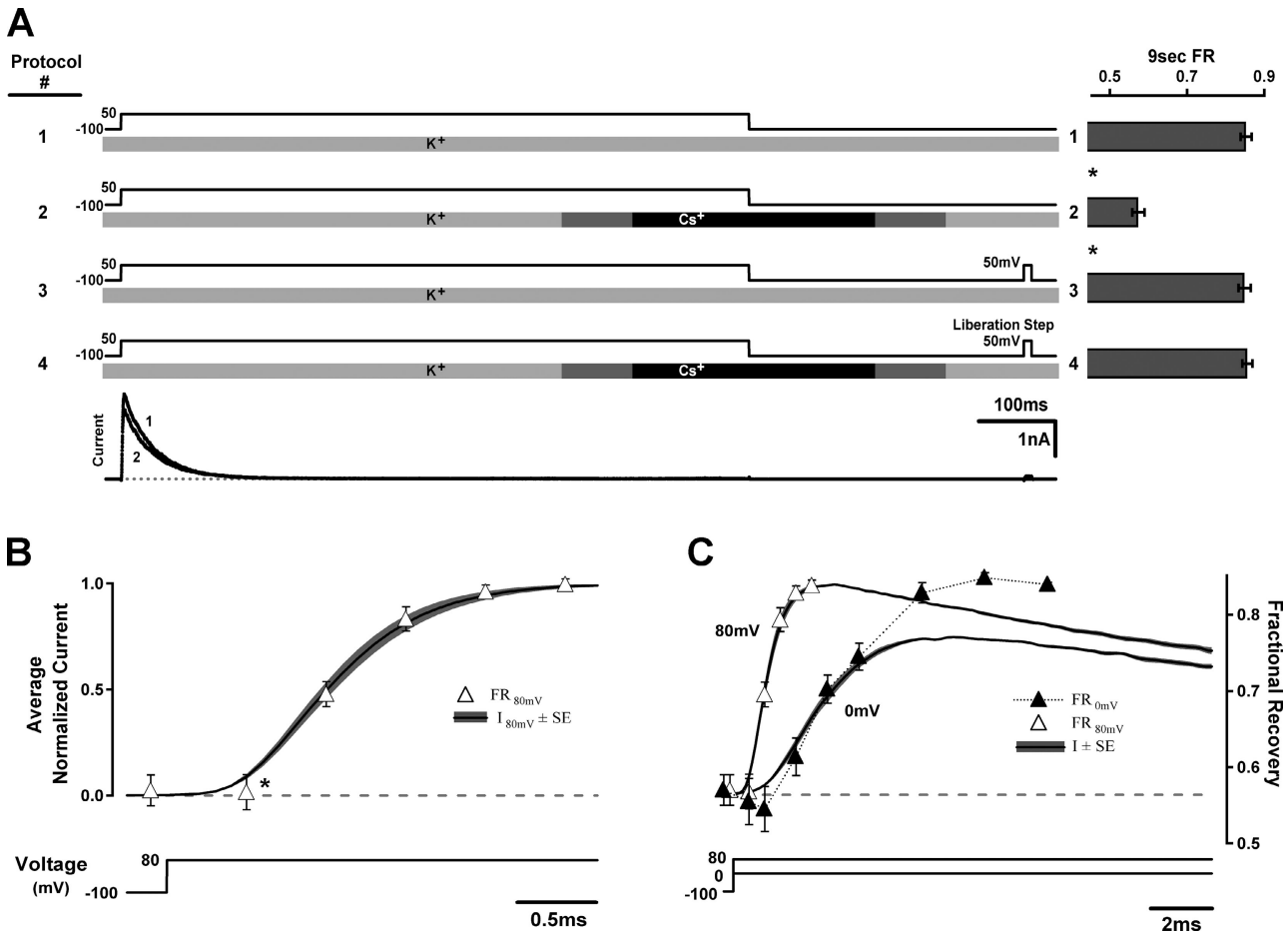

Figure 5. Activation gate-opening releases trapped Cs^+. 9-s FR was measured with a protocol similar to Fig. 4, Protocol 14, either with or without a brief depolarizing voltage step after Cs^+ washout to reopen the activation gate. (A) Protocols 1–3 show control voltage and perfusion protocols. Protocol 4 tests the ability of a 10-ms step to +50 mV to restore FR to Cs^+-free levels. As in Fig. 4, bars at right show resulting FR (n = 5–9). Asterisks mark significantly different adjacent pairs ($P < 0.05$). Current traces shown below were evoked by Protocol 4, where trace 1 shows the initial current amplitude, and trace 2 shows current after the 9-s recovery period. Note that most of the original current amplitude is regained in the second trace. (B) Comparison of recovery time course and channel activation kinetics at +80 mV. The black trace shows average current activation after a step to +80 mV (n = 6). Gray swaths on either side of the line represent standard error of the current amplitude. Open triangles show FR measured using a protocol similar to that shown in A, Protocol 4, except that the liberation step was increased to +80 mV, and step duration was varied from 0 to 2.5 ms (n = 5). The initial lag characteristic of *Shaker* activation is demarked with an asterisk. (C) Comparison of recovery time course and channel activation kinetics at 0 mV. To examine the time course of Cs^+ liberation at 0 mV, FR was measured after liberation steps lasting from 0 to 10 ms. Fractional recovery increased with step duration. Mean current during a step to 0 mV is shown as a black line, surrounded by standard error swaths (n = 7). Current initially rises at a rate similar to the increase in FR, but soon falls away because the rate of activation at 0 mV is comparable to inactivation (τ_{inact} = 33 ± 1 ms). Current and Cs^+ liberation (open triangles) at +80 mV are included as a point of reference. Average current after a step to 0 mV was normalized to +80 mV based on relative macroscopic conductance ($G_{0mV}/G_{80mV} \approx 0.75$).

is the rate of opening of the activation gate. The same experiment performed with a liberation voltage step to 0 mV confirms this conclusion. At 0 mV, activation occurred significantly more slowly than at +80 mV, as did the kinetics of Cs^+ liberation. The correlation between Cs^+ liberation and channel opening kinetics provides strong evidence that a depolarizing pulse releases trapped Cs^+ from inactivated channels by opening the channel's activation gate.

These results suggest that slow recovery occurs when Cs^+ is trapped between the channel's activation and inactivation gates. In contrast, K^+ does not slow recovery, either because it does not occupy this site or because, when in this site, it influences recovery differently. We next asked how other intracellular monovalent cations influence recovery.

Selectivity of the Modulatory Binding Site

The channel's permeation pathway includes both the selectivity filter and the central cavity (Doyle et al., 1998; Hille, 2001; Zhou et al., 2001), a 10-Å-wide aqueous vestibule located halfway through the lipid bilayer and thought to be accessible to the intracellular solution in the channel's open state (Jiang et al., 2002b). Both the

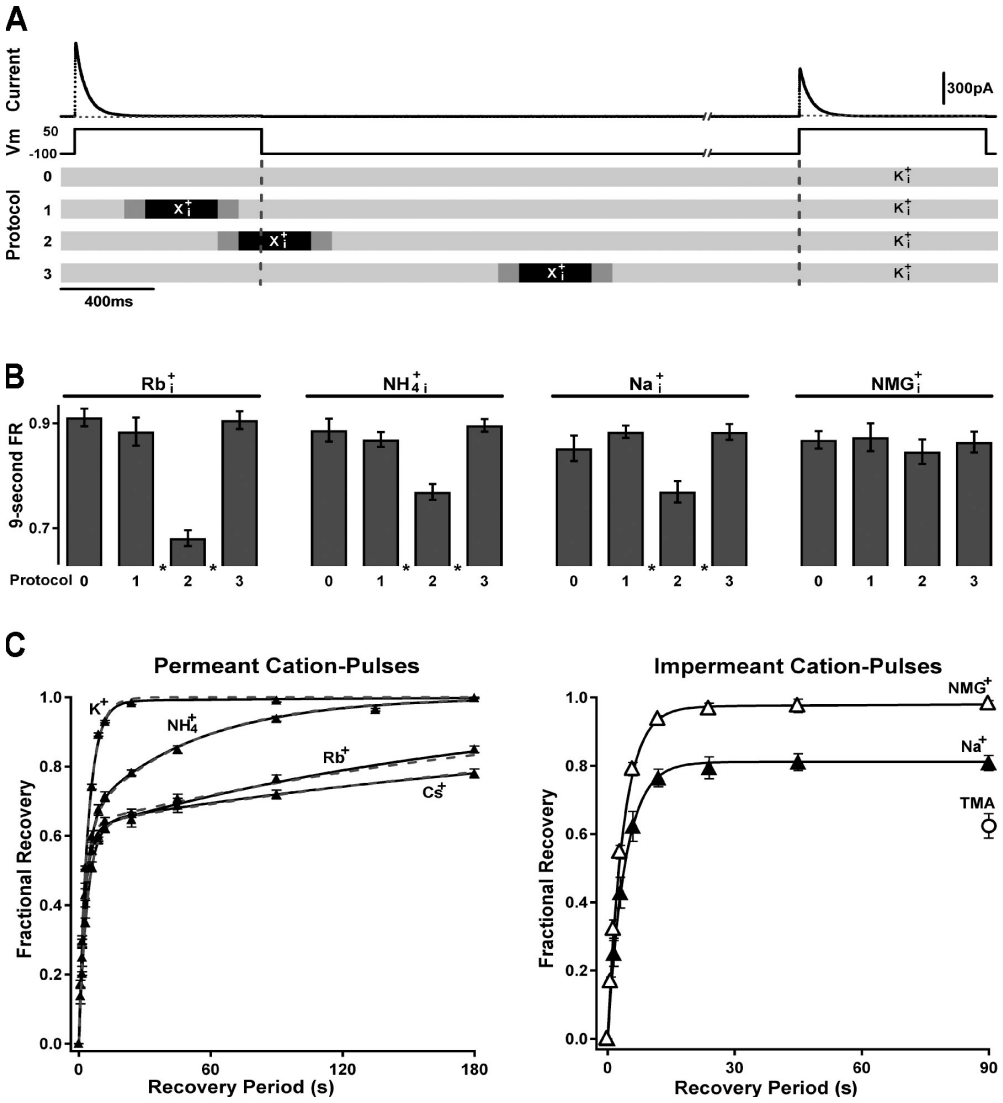

Figure 6. Influence of various intracellular ions on recovery. Inside-out patches containing 449K were studied in 20 mM K^+_o and perfused with 162 mM K^+_i and test cation pulses. (A) Perfusion protocols used to measure 9-s FR. (B) Average 9-s FR for channels pulsed with ~160 mM internal Rb^+, NH_4^+, Na^+, or NMG^+ using the protocols in A are represented as bars ± SEM (n = 4–7). Significantly different FR values ($P < 0.05$) are marked with asterisks. (C) Recovery kinetics after inactivation and a test cation pulse were examined using a protocol similar to Protocol 2 in A, but with a variable recovery period at −100 mV. Full recovery time courses (n = 3–5) are shown after pulses of either the permeant cations K^+_i, $NH_4^+{}_i$, Rb^+_i, or Cs^+_i (left), or pulses of the impermeant cations Na^+_i, NMG^+_i, or TMA_i (right). The TMA data represent the steady-state FR: the value is the same at 90 s (shown) and 180 s (not depicted), 0.64 ± 0.03 and 0.62 ± 0.02, respectively. Each curve was independently fit with the functions used for Fig. 1 and Table I (solid, black lines). For permeant cations, a global fit was performed in which a single value for τ_{fast}, A_{fast}, and A_{slow} was found for all curves and only τ_{slow} was allowed to vary from curve to curve (dashed, gray lines). Parameters for independent and global fits are shown in Table II.

selectivity filter and the central cavity exhibit ion selectivity (Neyton and Miller, 1988; Hille, 2001; Nimigean and Miller, 2002; Y. Zhou and MacKinnon, 2004). Because the binding site for the intracellular cation is within the permeation pathway (Figs. 3–5), we expect the modulatory binding site to be ion selective as well.

To probe the selectivity of the modulatory site, we measured recovery as a function of intracellular cation. Pulses of various intracellular cations were applied to inactivated 449K channels either at +50 mV, during the transition from +50 to −100 mV, or late in the recovery phase at −100 mV (Fig. 6 A). As with Cs^+_i, the other monovalent cations, Rb^+_i, $NH_4^+{}_i$, or Na^+_i, reduced FR when the cation pulse coincided with the transition from +50 to −100 mV, but had no effect when applied earlier or later in the protocol. Pulses of NMG^+_i did not change FR (Fig. 6 B). To examine the entire recovery time course for each test cation, we used a protocol similar to Protocol 2 in Fig. 6 A. The results are plotted in Fig. 6 C, along with the fits to a double-exponential function containing a fast and slow time constant (τ_{fast} and τ_{slow}) and weight coefficients, A_{fast} and A_{slow}, for the respective fast and slow phases of recovery. For permeant cations, K^+_i, $NH_4^+{}_i$, Rb^+_i, or Cs^+_i, regardless of the intracellular cation present when inactivated channels are returned to the hyperpolarized holding potential, τ_{fast}, A_{fast}, and A_{slow} for the recovery time courses are similar (Table II). The simultaneous fit to the time courses of all of the permeant cation pulse recoveries shown in Fig. 6 C demonstrates that the variation of a single parameter, τ_{slow}, is sufficient to account for each time course ($\chi^2 = 0.007$).

TABLE II

Cation-pulse Recovery Kinetics in 449K Shaker

Perfused Cation		Independent Fit			Global Fit		
		A_{slow}	τ_{fast} or τ_{rec} (s)	τ_{slow} (s)	A_{slow}	τ_{fast} (s)	τ_{slow} (s)
Permeant Cations	K^+_i	–	4.30 ± 0.03	–	0.37 ± 0.01	3.18 ± 0.16	6.78 ± 0.63
	$NH_4^+{}_i$	0.33 ± 0.01	3.25 ± 0.10	56 ± 3.2	0.37 ± 0.01	3.18 ± 0.16	47.0 ± 4.5
	Rb^+_i	0.38 ± 0.01	2.54 ± 0.19	201 ± 27	0.37 ± 0.01	3.18 ± 0.16	220 ± 28
	Cs^+_i	0.36 ± 0.01	3.81 ± 0.12	358 ± 32	0.37 ± 0.01	3.18 ± 0.16	355 ± 62
Impermeant Cations	Na^+_i	0.20 ± 0.02	3.93 ± 0.43	980 ± 650	–	–	–
	NMG^+_i	–	4.01 ± 0.02	–	–	–	–

Time courses were fit as described in Table I. See Fig. 6 C for description of global fit.

The invariance of A_{slow} indicates that the identity of the applied permeant cation does not influence the fraction of channels that recover slowly. However, the variation in the rate of recovery, $1/\tau_{slow}$, with type of intracellular cation is consistent with the hypothesis that a modulatory cation is trapped following return of channels to a hyperpolarized potential and that the nature of this trapped cation determines the recovery rate. Entrapment is supported by the fact that all of the non-K^+ permeant cations' slow recovery long after the intracellular solution is switched back to K^+. Slow recovery can be explained by one of two possible scenarios: the presence of a particular cation in the modulatory site, or by an empty modulatory site. The latter model can be eliminated based on the following considerations. First, raising Cs^+_i slows the recovery rate (Fig. 2), exactly the opposite result expected if empty modulatory sites promote slower recovery. Second, a model in which empty modulatory sites underlie slow recovery predicts that the rate of the slower component would be the same for all ion species, a prediction that is also in conflict with our data. This suggests that the fast recovery observed in the presence of K^+_i occurs not because K^+ fails to occupy the modulatory binding site, but because K^+, when trapped at this site, catalyzes recovery more effectively than do other cations. Consistent with this hypothesis, we interpret the similarity between the kinetics of recovery from channels bathed in bilateral K^+ (τ_{rec} = 4.3 s) and the fast phase of recovery after the application of other intracellular cations (τ_{fast} = 2.5–3.8 s) as representing the fraction of channels containing a trapped K^+ at the modulatory site.

The effect of intracellular impermeant cations, NMG^+ and Na^+, on recovery differs from that seen for permeant cations. The recovery time course after a pulse of NMG^+ displays monoexponential kinetics (τ_{rec} = 4.01 ± 0.02 s, Fig. 6 C) that closely resemble the recovery seen from channels bathed in K^+_i. These results indicate that NMG^+ does not stabilize a long-lived nonconducting state. Either a trapped NMG^+_i fails to bind to the modulatory site or NMG^+_i does not become trapped behind the activation gate. However, tetramethylammonium (TMA), a cation that can enter the channel from the intracellular compartment, but cannot permeate further into the selectivity filter, prevents recovery. When 160 mM TMA is applied to inactivated 449K channels using Protocol 2 shown in Fig. 6 A, FR is 0.64 ± 0.03 at 90 s and 0.62 ± 0.02 at 180 s (Fig. 6 C). When Na^+_i is applied, only 0.83 ± 0.01 of the original current amplitude is restored in the 180-s period during which recovery was examined. This time course is best fit with a bi-exponential function with τ_{fast} similar to that seen when K^+_i is applied (3.93 ± 0.43 s) and a very large τ_{slow} (980 ± 650 s). A_{slow} is small (0.20 ± 0.02) compared with that observed for permeant cations, suggesting that 80% of channels trap a K^+ and 20% trap Na^+ in the modulatory site. In the latter case, the channel does not recover (see Discussion, Fig. 8).

Our working hypothesis to explain these data is that inactivated channels, when returned to a hyperpolarized holding potential, trap a cation behind the activation gate. The ability of channels to return to a noninactivated state depends on the identity of the trapped cation, in the following rank order: $K^+ > NH_4^+ > Rb^+ > Cs^+ >> Na^+$, TMA.

DISCUSSION

Although the processes of permeation and gating occur on time scales that typically differ by more than five orders of magnitude, gate movement may be highly sensitive to permeant ions that transiently visit binding sites of the permeation pathway. The regulation of gating by permeant ions is highlighted in our study of the recovery from slow inactivation in *Shaker*. First, the rate of recovery depends upon the species of permeant ion present on the intracellular side of the channel. The recovery from inactivation at a hyperpolarized voltage is relatively rapid in the presence of internal K^+ and is slower if the channels are hyperpolarized in the presence of intracellular NH_4^+, Rb^+, Cs^+, Na^+, or TMA. Second, the ion dependence of recovery derives from entrapment of a cation within the permeation pathway, specifically between the channel's slow inactivation gate and the intracellular activation gate. This trapping is caused by activation

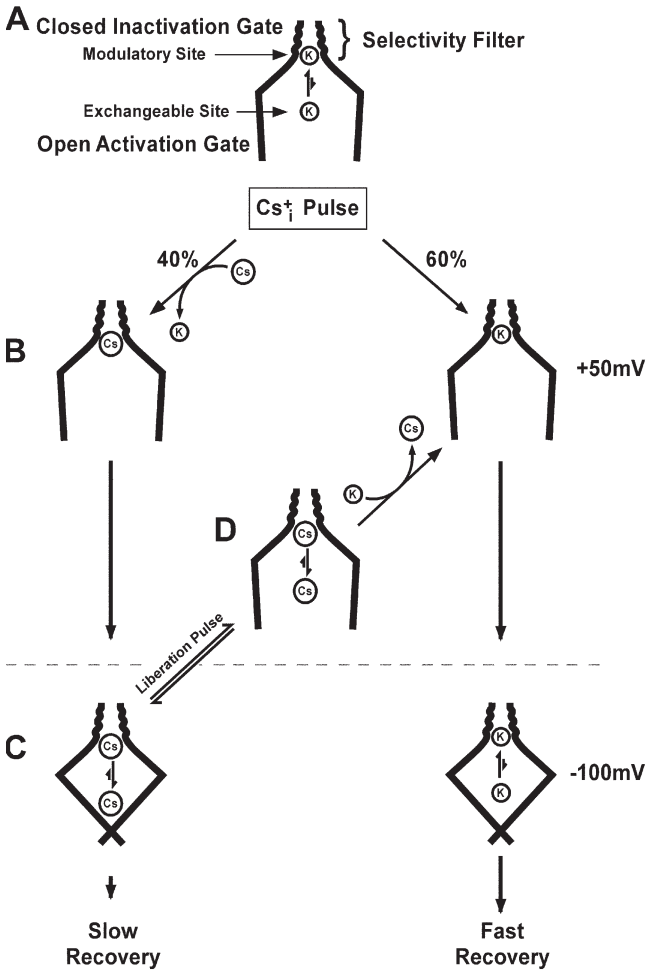

Figure 7. A model for intracellular cation interaction with the inactivated channel. A slow inactivated channel is represented by squiggled lines at the selectivity filter. The intracellular portion of the channel, including the cavity, is shown by straight lines. (A) Channels inactivated in the presence of K^+_i bind K^+ in either an exchangeable site or a modulatory site at the intracellular end of the selectivity filter. (B) When a Cs^+ pulse is applied intracellularly to depolarized, inactivated channels, K^+ in the exchangeable site is rapidly replaced by Cs^+. K^+ bound to the modulatory site (shown) exchanges very slowly. (C) Figures below dashed line represent structures occurring at −100 mV. After return to a hyperpolarized potential, the activation gate closes, and either Cs^+ or K^+ becomes trapped between the closed inactivation gate and the activation gate. Recovery is promoted by interaction of the trapped cation with the modulatory site. Channels in which K^+ is trapped recover quickly (contributing to the fast phase of the recovery time course), whereas channels with trapped Cs^+ recover slowly. (D) Trapped Cs^+ can be liberated from the channel by depolarization, which opens the activation gate, in the presence of K^+_i. Thus, Cs^+ re-exchanges for K^+, resulting in fast recovery.

gate closure upon repolarization of the channel. Fig. 7 proposes a mechanism involving cation movement between modulatory and exchangeable sites within the permeation pathway. This mechanism is largely consistent with our data and constitutes a framework for the following discussion.

Location of the Trapped Cation

Slow inactivation involves a rearrangement of the outer mouth of the channel and a portion of the selectivity filter (Grissmer and Cahalan, 1989b; Choi et al., 1991; Yellen et al., 1994; Liu et al., 1996; Starkus et al., 1997; Harris et al., 1998; Kiss et al., 1999; Ogielska and Aldrich, 1999; Larsson and Elinder, 2000; Wang et al., 2000). This rearrangement prevents the passage of ions across the selectivity filter. The conducting conformation of the selectivity filter includes five adjacent cation binding sites numbered 0 (outermost) through 4 (innermost) (Morais-Cabral et al., 2001). Although some of these sites may be disrupted when the channel inactivates, the conformational changes associated with slow inactivation appear to be localized to the more external binding sites (Ogielska and Aldrich, 1999; Zhou et al., 2001). Thus, selectivity filter binding sites such as site 4, and possibly site 3, may persist in the inactivated state (Harris et al., 1998; Jiang and MacKinnon, 2000; Lenaeus et al., 2005) and constitute the outermost possible site(s) for the location of entrapped modulatory cations. At the other end, the innermost boundary for the site of entrapment is the closed activation gate (Fig. 7 C). This is inferred from two observations. First, liberation of Cs^+ from inactivated channels at depolarized potentials tracks activation gate opening kinetics. Second, repolarization of the inactivated channel to −120 mV closes the activation gate with a time constant of ∼23 ms (Panyi, G., and C. Deutsch. 2006. *Biophys. J.* 90:243a), consistent with our observation that the period during which channel recovery is maximally sensitive to intracellular cations lasts no more than 200 ms after return of depolarized channels to their holding potential. Thus, activation gate transitions are likely to be responsible for both the entrapment and the release of the cation.

The activation gate is formed by the bundle crossing of each of the four subunit's S6 transmembrane helices at the intracellular side of the channel's pore domain (Liu et al., 1997; Doyle et al., 1998; Jiang et al., 2002a). After closure of the gate, the channel retains a 10-Å-wide aqueous cavity between the selectivity filter and the S6 helix bundle (Doyle et al., 1998). Near the center of this cavity is a site for monovalent cations, including Tl^+, K^+, Rb^+, Cs^+, and Na^+ (Y. Zhou and MacKinnon, 2004). A cation residing in this cavity site is expected to be readily exchangeable when the activation gate is open. Cs^+ has the additional ability to occupy a position between site 4 and the central cavity site, though occupancy of this site is likely to be mutually exclusive with both site 4 and the central cavity site (Y. Zhou and MacKinnon, 2004). Because this site is located near site 4 (but more intracellular), we refer to it as site 4' (M. Zhou and MacKinnon, 2004). Site 4' may be the site through which Cs^+_i and Rb^+_i, but not K^+_i, compete with the binding of the intracellular channel blocker, TBSb

(Thompson and Begenisich, 2003). We propose that the modulatory site is at 4 or 4' and that the exchangeable site is either here or at a more intracellular site, perhaps in the center of the cavity (Fig. 7 A). Cations in either of these sites become trapped when the activation gate closes.

Mechanism of Ion-sensitive Recovery

Upon inactivation, channels bind K^+ in the modulatory site (Fig. 7 A). K^+ occupancy of this site promotes recovery. When Cs^+_i is applied to channels with an open activation gate, replacement of K^+ with Cs^+ requires departure of K^+ from the modulatory site. A closed inactivation gate presumably precludes outward movement of a K^+ ion through the selectivity filter. Therefore, the exchange of Cs^+ for K^+ must occur through the open activation gate. We propose that the exit rate of K^+ from the modulatory site is significantly slower in the inactivated channel than in the noninactivated channel due to a higher K^+ affinity in the inactivated channel. This explains the observed biphasic recovery shown in Fig. 6 C. After repolarization of inactivated channels during a non-K^+ permeant cation pulse, ~60% of channels recover quickly, with a rate nearly identical to that seen in K^+_i. The other 40% of channels recover with a rate that depends on the identity of the cation applied during the hyperpolarization transition. The fast recovery route taken by 60% of the channels is depicted by the right column of steps in Fig. 7. The slower route for the remaining 40% is depicted by the left column of transitions. The slow, rate-limiting exit rate for K^+ from the modulatory site explains why a fixed fraction of channels successfully exchange K^+ with a perfused permeant cation, and why this fraction (0.4) is independent of the species of non-K^+ permeant cation applied.

Although the rate of K^+ exit from the channel may be slow relative to activation gate transitions, the rate of Cs^+ exit is not, as suggested by our finding that the rate-limiting step in Cs^+ liberation is opening of the activation gate. The faster rate of exit for Cs^+ may be explained by its low affinity for the modulatory site. For example, Cs^+ may prefer to occupy a site similar to site 4' or the central cavity site, rather than site 4. Regardless of which site Cs^+ occupies, washout from that site is fast relative to opening of the activation gate (Fig. 5 and Fig. 7 D).

Further support for an intimate relationship between permeation and recovery is evident from the monotonic relationship between rate of recovery and open channel conductance (Fig. 8 A). We speculate that a permeant ion in the modulatory binding site of an inactivated channel (I) moves from the modulatory site to a deeper location (in state NI [noninactivated]) within the selectivity filter for the channel to recover (Fig. 8 B). I' is a transient state that resembles a conductive state with respect to the structure of the selectivity filter. Recovery in this model occurs when the ion in state I' hops further into the selectivity filter, thus stabilizing the NI state. In an open channel, the relative ability of an ion to move easily from one site to another is manifest as its conductance. The correlation between the recovery rate and conductance suggests that the I'-to-NI transition is common to both processes. Thus, a highly conductive cation like K^+ is expected to promote more rapid recovery than a less conductive ion. If an ion does not move rapidly enough from the modulatory site in I' to the second site in NI, the channel will rapidly return to state I. In this model, therefore, the cation selectivity sequence for recovery should correlate with conductance. Our model (Figs. 7 and 8) suggests that an ion like Cs^+, when bound in the modulatory site, dissociates more rapidly than K^+ into the cavity, but slower than K^+ into the selectivity filter (the I'-to-NI transition). This is simply explained if K^+ has a higher affinity for the modulatory site than Cs^+, but that the energy barrier for Cs^+ to move deeper (more extracellular) into the selectivity filter is much higher than the comparable barrier for K^+. This is consistent with the higher K^+ selectivity of sites deeper into the selectivity filter (Aqvist and Luzhkov, 2000; Berneche and Roux, 2001; Noskov et al., 2004).

Moreover, the model shown in Fig. 8 B can explain the results obtained with internal Na^+ (Fig. 6 C). Only ~20% of the channels trap Na^+ ion when hyperpolarized in the presence of Na^+_i due to the relatively poor selectivity of the most intracellular selectivity filter sites, for example, sites 3 and 4 (Aqvist and Luzhkov, 2000; Berneche and Roux, 2001; Noskov et al., 2004). Once in this modulatory site, Na^+ does not move readily into the more extracellular site of state NI. This is consistent with the fact that sodium is nearly impermeant, having a conductance in *Shaker* that is indistinguishable from leak (Heginbotham and MacKinnon, 1993). Thus, there is no recovery on the time scale of our measurements. The rapid 80% recovery is from inactivated channels that have trapped a K^+ ion. Similarly, the lack of recovery by inactivated channels that have trapped a TMA ion during a TMA-pulse is consistent with the model proposed in Fig. 8 B.

Occupancy of the selectivity filter by permeant cations is likely to be necessary for the maintenance of a conductive conformation. The presence of permeant cations in the selectivity filter has been suggested to be necessary to counterbalance the electrostatic repulsion experienced by opposing selectivity filter oxygen atoms as a consequence of their negative dipoles (Almers and Armstrong, 1980; Shrivastava and Sansom, 2000; Zhou et al., 2001). At low permeant cation concentrations, the selectivity filter binding sites are not fully occupied and the selectivity filter is distorted (Shrivastava and Sansom, 2000; Morais-Cabral et al., 2001; Zhou et al.,

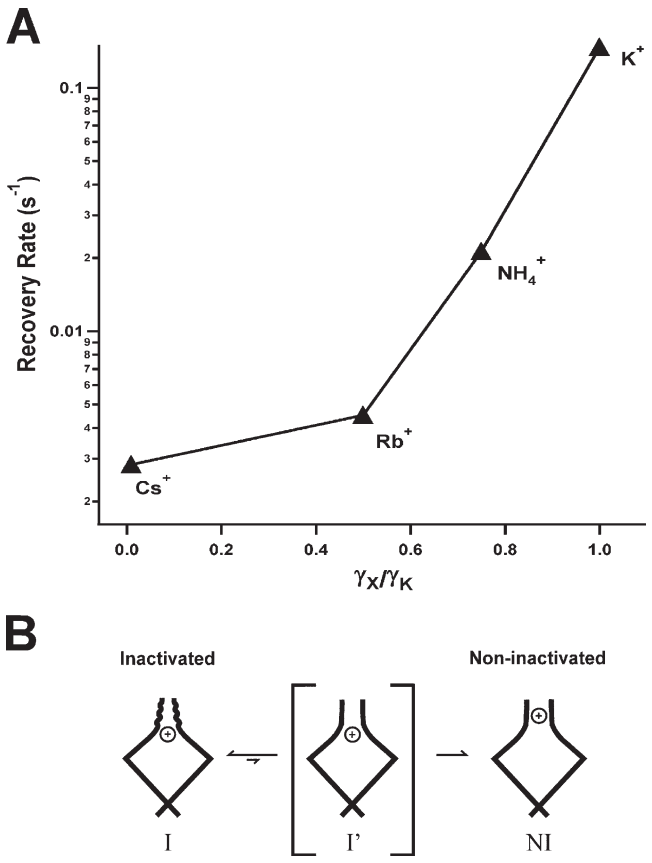

Figure 8. Conductance vs. recovery rate. (A) Rate constants from the slow phase of recovery derived from Fig. 6 C are plotted as a function of the single-channel conductance ratio for each of the indicated cations. Conductance data are from Heginbotham and MacKinnon (1993), measured in T449 *Shaker*-IR. Data for K^+, Rb^+, or NH_4^+ are from single channel currents. Cs^+ conductance was calculated using nonstationary fluctuation analysis because the small conductance of Cs^+ (0.32 pS) precluded single channel current recording. We used nonstationary fluctuation analysis to confirm that mutation of T449 to A or V does not change γ_{Cs}/γ_K (not depicted). γ_{Cs} in 449K could not be measured due to its rapid inactivation and entry into the long-lived nonconducting state in the presence of Cs^+. (B) A model describing how a trapped permeant cation may promote recovery. In the inactivated channel (I), a cation is bound to a modulatory site. The inactivated channel transiently reverts to the noninactivated conformation (I'), a state that is unstable in the absence of a cation bound in the selectivity filter. Only when the trapped cation moves into the selectivity filter does the NI state become stable, resulting in recovery. The relative rates for these transitions are indicated by the length of the arrows.

2001; Zhou and MacKinnon, 2003). A possible consequence of removal of permeant cations from the channel, therefore, is entry into a stable nonconducting conformation (Melishchuk et al., 1998; Loboda et al., 2001). Underpopulation of at least some selectivity filter binding sites may also be characteristic of the slow inactivated state (Lopez-Barneo et al., 1993; Baukrowitz and Yellen, 1995; Rasmusson et al., 1995; Baukrowitz and Yellen, 1996; Levy and Deutsch, 1996a,b; Molina et al., 1997; Kiss and Korn, 1998; Molina et al., 1998; Fedida et al., 1999; Ogielska and Aldrich, 1999), and refilling of these sites may be required for recovery (Berneche and Roux, 2005).

Further Implications for K_V Channel Gating

Cation trapping during the repolarization transition has important implications for the nature of activation gate movement in inactivated channels. First, the findings that depolarization liberates a cation trapped by the activation gate and that Cs^+ liberation tracks activation kinetics of the noninactivated channel suggests that activation gate opening at voltages between 0 and +80 mV is not influenced strongly by either inactivation or a trapped Cs^+ ion. Our results are inconsistent with the previous speculation that large cations, including Cs^+, must exit the central cavity before activation gate closure (Melishchuk and Armstrong, 2001). However, our results are consistent with crystal structures of *KcsA* in which a channel with a closed activation gate retains enough room in the central cavity for a permeant cation, including Cs^+ (Y. Zhou and MacKinnon, 2004), as well as larger cationic blockers (Lenaeus et al., 2005). We conclude that slow-inactivated channels can accommodate permeant cations behind the closed activation gate.

A second implication from our studies pertains to the role of the 449 side chain in K^+ channel gating. This side chain influences both entry into (Lopez-Barneo et al., 1993; Molina et al., 1997) and recovery from (Rasmusson et al., 1995; Meyer and Heinemann, 1997) the inactivated state. We find that the influence of the trapped cation on recovery rate also depends on the 449 side chain. It is possible that recovery reflects a ternary interaction in which the 449 side chain governs cation binding to an extracellular site, which in turn affects the interaction between trapped intracellular cations and the selectivity filter. Another possibility is that the 449 side chain determines how inactivation-associated rearrangements at the outer mouth of the channel influence the stability of ion binding sites within the selectivity filter. Although the mechanism remains unclear, it is certain that 449 plays an important role in governing both entry into and recovery from inactivation. The lack of conservation of this side chain among K^+ channels contributes to the physiological diversity of K^+ channel function.

Recovery from the slow inactivated state is a critical gating process. It determines the number of K^+ channels available to maintain excitable cells at a negative resting potential, ultimately dictating cellular excitability. Maintenance of a conducting conformation appears to require bound permeant cations and, because K^+ channels have evolved to coordinate K^+ ions, these cations are the most effective at accomplishing this task. In addition to this prerequisite for permeation, we now

include one for gating, specifically for recovery. Binding of permeant cations to sites in the permeation pathway stabilizes rearrangements in the channel protein that appear to be necessary for recovery from the slow-inactivated state.

We thank Dr. R. Horn for critical reading of the manuscript and technical advice, Dr. G. Panyi for thoughtful discussion and help with analysis, and Drs. C. Miller and B. Roux for suggestions.

This work was supported by National Institutes of Health grant GM 069837 and National Research Service Award HL-07027.

Olaf S. Andersen served as editor.

Submitted: 14 April 2006
Accepted: 30 June 2006

REFERENCES

Aqvist, J., and V. Luzhkov. 2000. Ion permeation mechanism of the potassium channel. *Nature.* 404:881–884.

Almers, W., and C.M. Armstrong. 1980. Survival of K^+ permeability and gating currents in squid axons perfused with K^+-free media. *J. Gen. Physiol.* 75:61–78.

Armstrong, C.M. 1969. Inactivation of the potassium conductance and related phenomena caused by quaternary ammonium ion injection in squid axons. *J. Gen. Physiol.* 54:553–575.

Baukrowitz, T., and G. Yellen. 1995. Modulation of K+ current by frequency and external [K+]: a tale of two inactivation mechanisms. *Neuron.* 15:951–960.

Baukrowitz, T., and G. Yellen. 1996. Use-dependent blockers and exit rate of the last ion from the multi-ion pore of a K+ channel. *Science.* 271:653–656.

Berneche, S., and B. Roux. 2001. Energetics of ion conduction through the K+ channel. *Nature.* 414:73–77.

Berneche, S., and B. Roux. 2005. A gate in the selectivity filter of potassium channels. *Structure.* 13:591–600.

Choi, K.L., R.W. Aldrich, and G. Yellen. 1991. Tetraethylammonium blockade distinguishes two inactivation mechanisms in voltage-activated K+ channels. *Proc. Natl. Acad. Sci. USA.* 88:5092–5095.

Ding, S., and R. Horn. 2002. Tail end of the S6 segment: role in permeation in Shaker potassium channels. *J. Gen. Physiol.* 120:87–97.

Doyle, D.A., J. Morais Cabral, R.A. Pfuetzner, A. Kuo, J.M. Gulbis, S.L. Cohen, B.T. Chait, and R. MacKinnon. 1998. The structure of the potassium channel: molecular basis of K+ conduction and selectivity. *Science.* 280:69–77.

Fedida, D., N.D. Maruoka, and S. Lin. 1999. Modulation of slow inactivation in human cardiac Kv1.5 channels by extra- and intracellular permeant cations. *J. Physiol.* 515:315–329.

Grissmer, S., and M. Cahalan. 1989a. Divalent ion trapping inside potassium channels of human T lymphocytes. *J. Gen. Physiol.* 93:609–630.

Grissmer, S., and M. Cahalan. 1989b. TEA prevents inactivation while blocking open K+ channels in human T lymphocytes. *Biophys. J.* 55:203–206.

Harris, R.E., H.P. Larsson, and E.Y. Isacoff. 1998. A permanent ion binding site located between two gates of the Shaker K+ channel. *Biophys. J.* 74:1808–1820.

Heginbotham, L., and R. MacKinnon. 1993. Conduction properties of the cloned Shaker K+ channel. *Biophys. J.* 65:2089–2096.

Hille, B. 2001. Ion Channels of Excitable Membranes. Third edition. Sinauer Associates, Inc., Sunderland, MA. 814 pp.

Holmgren, M., M.E. Jurman, and G. Yellen. 1996. N-type inactivation and the S4-S5 region of the Shaker K^+ channel. *J. Gen. Physiol.* 108:195–206.

Hoshi, T., W.N. Zagotta, and R.W. Aldrich. 1990. Biophysical and molecular mechanisms of Shaker potassium channel inactivation. *Science.* 250:533–538.

Hoshi, T., W.N. Zagotta, and R.W. Aldrich. 1991. Two types of inactivation in Shaker K+ channels: effects of alterations in the carboxy-terminal region. *Neuron.* 7:547–556.

Hoshi, T., W.N. Zagotta, and R.W. Aldrich. 1994. Shaker potassium channel gating. I: Transitions near the open state. *J. Gen. Physiol.* 103:249–278.

Jiang, Y., and R. MacKinnon. 2000. The barium site in a potassium channel by X-ray crystallography. *J. Gen. Physiol.* 115:269–272.

Jiang, Y., A. Lee, J. Chen, M. Cadene, B.T. Chait, and R. MacKinnon. 2002a. Crystal structure and mechanism of a calcium-gated potassium channel. *Nature.* 417:515–522.

Jiang, Y., A. Lee, J. Chen, M. Cadene, B.T. Chait, and R. MacKinnon. 2002b. The open pore conformation of potassium channels. *Nature.* 417:523–526.

Jurman, M.E., L.M. Boland, and G. Yellen. 1994. Visual identification of individual transfected cells for electrophysiology using antibody-coated beads. *Biotechniques.* 17:876–881.

Kiss, L., and S.J. Korn. 1998. Modulation of C-Type inactivation by K+ at the potassium channel selectivity filter. *Biophys. J.* 74:1840–1849.

Kiss, L., J. LoTurco, and S.J. Korn. 1999. Contribution of the selectivity filter to inactivation in potassium channels. *Biophys. J.* 76:253–263.

Kozak, M. 1991. Structural features in eukaryotic mRNAs that modulate the initiation of translation. *J. Biol. Chem.* 266: 19867–19870.

Kurata, H.T., Z. Wang, and D. Fedida. 2004. NH_2-terminal inactivation peptide binding to C-type-inactivated Kv channels. *J. Gen. Physiol.* 123:505–520.

Larsson, H.P., and F. Elinder. 2000. A conserved glutamate is important for slow inactivation in K+ channels. *Neuron.* 27:573–583.

Lenaeus, M.J., M. Vamvouka, P.J. Focia, and A. Gross. 2005. Structural basis of TEA blockade in a model potassium channel. *Nat. Struct. Mol. Biol.* 12:454–459.

Levy, D.I., and C. Deutsch. 1996a. Recovery from C-type inactivation is modulated by extracellular potassium. *Biophys. J.* 70:798–805.

Levy, D.I., and C. Deutsch. 1996b. A voltage-dependent role for K+ in recovery from C-type inactivation. *Biophys. J.* 71:3157–3166.

Liu, Y., M.E. Jurman, and G. Yellen. 1996. Dynamic rearrangement of the outer mouth of a K+ channel during gating. *Neuron.* 16:859–867.

Liu, Y., M. Holmgren, M.E. Jurman, and G. Yellen. 1997. Gated access to the pore of a voltage-dependent K+ channel. *Neuron.* 19:175–184.

Loboda, A., A. Melishchuk, and C. Armstrong. 2001. Dilated and defunct K channels in the absence of K+. *Biophys. J.* 80:2704–2714.

Loots, E., and E.Y. Isacoff. 1998. Protein rearrangements underlying slow inactivation of the Shaker K^+ channel. *J. Gen. Physiol.* 112:377–389.

Lopez-Barneo, J., T. Hoshi, S.H. Heinemann, and R.W. Aldrich. 1993. Effects of external cations and mutations in the pore region on C-type inactivation of Shaker potassium channels. *Receptors Channels.* 1:61–71.

Margolskee, R.F., P. Kavathas, and P. Berg. 1988. Epstein-Barr virus shuttle vector for stable episomal replication of cDNA expression libraries in human cells. *Mol. Cell. Biol.* 8:2837–2847.

Margolskee, R.F., B. McHendry-Rinde, and R. Horn. 1993. Panning transfected cells for electrophysiological studies. *Biotechniques.* 15:906–911.

Melishchuk, A., and C.M. Armstrong. 2001. Mechanism underlying slow kinetics of the OFF gating current in Shaker potassium channel. *Biophys. J.* 80:2167–2175.

Melishchuk, A., A. Loboda, and C.M. Armstrong. 1998. Loss of Shaker K channel conductance in 0 K+ solutions: role of the voltage sensor. *Biophys. J.* 75:1828–1835.

Meyer, R., and S.H. Heinemann. 1997. Temperature and pressure dependence of Shaker K+ channel N- and C-type inactivation. *Eur. Biophys. J.* 26:433–445.

Molina, A., A. Castellano, and J. Lopez-Barneo. 1997. Pore mutations in Shaker K+ channels distinguish between the sites of tetraethylammonium blockade and C-type inactivation. *J. Physiol.* 499:361–367.

Molina, A., P. Ortega-Saenz, and J. Lopez-Barneo. 1998. Pore mutations alter closing and opening kinetics in Shaker K+ channels. *J. Physiol.* 509:327–337.

Morais-Cabral, J.H., Y. Zhou, and R. MacKinnon. 2001. Energetic optimization of ion conduction rate by the K+ selectivity filter. *Nature.* 414:37–42.

Neyton, J., and C. Miller. 1988. Discrete Ba^{2+} block as a probe of ion occupancy and pore structure in the high-conductance Ca^{2+}-activated K^+ channel. *J. Gen. Physiol.* 92:569–586.

Nimigean, C.M., and C. Miller. 2002. Na^+ block and permeation in a K^+ Channel of Known Structure. *J. Gen. Physiol.* 120:323–335.

Noskov, S.Y., S. Berneche, and B. Roux. 2004. Control of ion selectivity in potassium channels by electrostatic and dynamic properties of carbonyl ligands. *Nature.* 431:830–834.

Ogielska, E.M., and R.W. Aldrich. 1999. Functional consequences of a decreased potassium affinity in a potassium channel pore. Ion interactions and C-type inactivation. *J. Gen. Physiol.* 113:347–358.

Pardo, L.A., S.H. Heinemann, H. Terlau, U. Ludewig, C. Lorra, O. Pongs, and W. Stühmer. 1992. Extracellular K+ specifically modulates a rat brain K+ channel. *Proc. Natl. Acad. Sci. USA.* 89:2466–2470.

Rasmusson, R.L., M.J. Morales, R.C. Castellino, Y. Zhang, D.L. Campbell, and H.C. Strauss. 1995. C-type inactivation controls recovery in a fast inactivating cardiac K+ channel (Kv1.4) expressed in Xenopus oocytes. *J. Physiol.* 489(Pt 3):709–721.

Rasmusson, R.L., M.J. Morales, S. Wang, S. Liu, D.L. Campbell, M.V. Brahmajothi, and H.C. Strauss. 1998. Inactivation of voltage-gated cardiac K+ channels. *Circ. Res.* 82:739–750.

Shrivastava, I.H., and M.S.P. Sansom. 2000. Simulations of ion permeation through a potassium channel: molecular dynamics of KcsA in a phospholipid bilayer. *Biophys. J.* 78:557–570.

Starkus, J.G., L. Kuschel, M.D. Rayner, and S.H. Heinemann. 1997. Ion conduction through C-type inactivated Shaker channels. *J. Gen. Physiol.* 110:539–550.

Swenson, R.P., Jr., and C.M. Armstrong. 1981. K+ channels close more slowly in the presence of external K+ and Rb+. *Nature.* 291:427–429.

Thompson, J., and T. Begenisich. 2003. Functional identification of ion binding sites at the internal end of the pore in Shaker K+ channels. *J. Physiol.* 549:107–120.

Wang, Z., J.C. Hesketh, and D. Fedida. 2000. A high-Na(+) conduction state during recovery from inactivation in the K(+) channel Kv1.5. *Biophys. J.* 79:2416–2433.

Yellen, G., D. Sodickson, T.Y. Chen, and M.E. Jurman. 1994. An engineered cysteine in the external mouth of a K+ channel allows inactivation to be modulated by metal binding. *Biophys. J.* 66:1068–1075.

Zagotta, W.N., and R.W. Aldrich. 1990. Voltage-dependent gating of Shaker A-type potassium channels in *Drosophila* muscle. *J. Gen. Physiol.* 95:29–60.

Zagotta, W.N., T. Hoshi, and R.W. Aldrich. 1994a. Shaker potassium channel gating. III: Evaluation of kinetic models for activation. *J. Gen. Physiol.* 103:321–362.

Zagotta, W.N., T. Hoshi, J. Dittman, and R.W. Aldrich. 1994b. Shaker potassium channel gating. II: Transitions in the activation pathway. *J. Gen. Physiol.* 103:279–319.

Zhou, M., and R. MacKinnon. 2004. A mutant KcsA K^+ channel with altered conduction properties and selectivity filter ion distribution. *J. Mol. Biol.* 338:839–846.

Zhou, Y., and R. MacKinnon. 2003. The occupancy of ions in the K+ selectivity filter: charge balance and coupling of ion binding to a protein conformational change underlie high conduction rates. *J. Mol. Biol.* 333:965–975.

Zhou, Y., and R. MacKinnon. 2004. Ion binding affinity in the cavity of the KcsA potassium channel. *Biochemistry.* 43:4978–4982.

Zhou, Y., J.H. Morais-Cabral, A. Kaufman, and R. MacKinnon. 2001. Chemistry of ion coordination and hydration revealed by a K+ channel-Fab complex at 2.0 Å resolution. *Nature.* 414:43–48.